

IMECE2003-41958

CONFIGURATION ANALYSIS OF A NOVEL ZERO CO₂ EMISSION CYCLE WITH LNG CRYOGENIC EXERGY UTILIZATION

Na Zhang*

Institute of Engineering Thermophysics, Chinese Academy of Sciences
Beijing 100080, P. R. China

Noam Lior

Department of Mechanical Engineering and Applied Mechanics
University of Pennsylvania
Philadelphia, PA 19104-6315, USA

ABSTRACT

A novel liquefied natural gas (LNG) fueled power plant is proposed, which has virtually zero CO₂ and other emissions and a high efficiency. Natural gas is fired in highly enriched oxygen and recycled CO₂ flue gas. The plant operates in a quasi-combined cycle mode with a supercritical CO₂ Rankine-like cycle and a CO₂ Brayton cycle, interconnected by the heat transfer process in the recuperation system. By coupling with the LNG evaporation system as the cycle cold sink, the cycle condensation process can be achieved at a temperature much lower than ambient, and high-pressure liquid CO₂ ready for disposal can be withdrawn from the cycle without consuming additional power. The net thermal and exergy efficiencies of a base-case cycle are found to be over 65% and 50% respectively, which can be increased up to 68% and 54% when reheat is used. Cycle variants incorporating reheat, intercooling, and reheat+intercooling, as well as no use of LNG coldness, are also defined and analyzed for comparison. The approximate heat transfer area needed for the different cycle variants is also computed. Besides electricity and condensed CO₂, the byproducts of the plant are H₂O, liquid N₂ and Ar.

Keywords: Thermal cycle, near-zero CO₂ emission, LNG cryogenic exergy

NOMENCLATURE

A Heat exchanger surface area [m²]

e	Specific exergy [kJ/kg]
G	Mass flow rate [kg/s]
H_u	Fuel LHV value [kJ/kg]
h	Specific enthalpy [kJ/kg]
P	Pressure [bar]
R_g	Mass flow rate ratio of Brayton cycle [%], Eq. (4)
T	Temperature [K]
t	Temperature [°C]
s	Specific entropy [kJ/kg·K]
Q	Heat duty [MW]
U	Overall heat transfer coefficient [W/m ² ·K]
W	Power output [MW]
w	Specific power output [kJ/kg]
ΔT_p	Pinch point temperature difference [°C]
η_1	Thermal efficiency
η_2	Exergy efficiency

Subscripts

f	Fuel
h	High pressure
m	Intermediary pressure
L	Liquefied natural gas
l	Low pressure
1...30	States on the cycle flow sheet

* Corresponding author: Phone: +86 10 62561887 Fax: +86 10 62575913
E-mail: zhangna@mail.etp.ac.cn

INTRODUCTION

Liquefied natural gas (LNG) is regarded as a relatively clean energy resource. During the process of its preparation, approximately 500 kWh energy per ton LNG is consumed for compression and refrigeration and a considerable portion of this invested exergy is preserved in the LNG [1], which has a final temperature of about 110K, much lower than that of the ambient or of seawater. The liquefaction reduces its volume 600-fold, and thus makes long distance transportation convenient.

LNG is loaded into insulated tankers and transported to receiving terminals, where it is off-loaded and first pumped to certain pressure, and then re-vaporized and heated, by contact with seawater or with ambient air, to approximately ambient temperature for pipeline transmission to the consumers. It is thus possible to withdraw cryogenic exergy from the LNG evaporation process which otherwise will be wasted by seawater heating. This can be achieved with a properly designed thermal power cycle using the LNG evaporator as the cold sink [1-13].

Use of the cryogenic exergy of LNG for power generation includes methods which use the LNG as the working fluid in natural gas direct expansion cycles, or its coldness as the heat sink in closed-loop Rankine cycles [1-5], Brayton cycles [6-9], and combinations thereof [10, 11]. Other methods use the LNG coldness to improve the performance of conventional thermal power cycles. For example, LNG vaporization can be integrated with gas turbine inlet air cooling [5, 12] or steam turbine condenser system (by cooling the recycled water [11]), etc. Some pilot plants have been established in Japan from the 1970's, combining closed-loop Rankine cycles (with pure or mixture organic working fluids) and direct expansion cycles [1].

Increasing concern about greenhouse effects on climatic change prompted a significant growth in research and practice of CO₂ emission mitigation in recent years. The technologies available for CO₂ capture in power plants are mainly physical and chemical absorption, cryogenic fractionation, and membrane separation. The amount of energy needed for CO₂ capture could lead to the reduction of power generation efficiency by up to 10 percentage points [14, 15].

Besides the efforts for reduction of CO₂ emissions from existing power plants, concepts of power plants with zero CO₂ emission were proposed and studied. Particular attention has been paid to the research of trans-critical CO₂ cycle with fuel burning in highly enriched oxygen (99.5%+) and recycled CO₂ from the flue gas [16-25]. The common features of these cycles are the use of CO₂ as the working fluid and O₂ as the fuel oxidizer, produced by an air separation unit. With CO₂ condensation at a pressure of 60~70 bar (temperature 20~30°C), efficiencies of 0.35-0.49 were reported for plants based on such cycles, despite the additional power use for O₂ production and CO₂ condensation. Staivocivi [26] proposed an improvement to these cycles by coupling with a thermal absorption technology to lower the CO₂ condensation below ambient temperature (30bar, -5.5°C), and estimated a net power efficiency of 54%.

In a proposal by Velautham et al [13], an LNG evaporation system is included in a gas-steam combined power plant just for captured CO₂ liquefaction and for air separation to provide oxygen for gas combustion. Deng et al [9] proposed a gas turbine cycle with nitrogen as its main working fluid. The stoichiometric amount of air needed for the combustion is introduced at the compressor inlet, and mixed with the nitrogen. The turbine exhaust contains mainly nitrogen, combustion generated CO₂, and H₂O. With the cycle exothermic process being integrated with the LNG evaporation process, CO₂ and H₂O are separated from the main stream by change of their phase, from gas to solid and liquid states, respectively, and the

extra nitrogen is discharged. The main merit of this cycle is the absence of the air separation unit, but the combustion product may contain NO_x as well, and the collection and removal of solidified CO₂ may be difficult.

In this paper, a novel zero emission CO₂ capture system is proposed and thermodynamically modeled. The plant is operated by a CO₂ quasi-combined two-stage turbine cycle with methane burning in an oxygen and recycled-CO₂ mixture. Compared to the previous works, two new features are developed in this study: the first is the integration with an LNG evaporation process. As a result, the CO₂ condensation and cycle heat sink are at temperatures much lower than ambient. The second one is the thermal cross-integration of the CO₂ Rankine-like cycle and Brayton cycle inside the recuperation system, so the heat transfer related irreversibility could be reduced to improve the global plant efficiency. Our cycle has both high power generation efficiency and extremely low environmental impact. Further, variations of the cycle which incorporate intercooling, reheat, and both, as well as comparison to a similar cycle which doesn't use LNG coldness, are also described and analyzed.

THE CYCLE CONFIGURATION

The base-case cycle layout and the corresponding *t-s* diagram are shown in Fig. 1 and 2 respectively. Variations on this cycle are described and analyzed further below. It follows the well-established general principle of a topping Brayton cycle (working fluid here is CO₂/H₂O; *TIT*=1300°C), with heat recovery in a bottoming supercritical CO₂ Rankine cycle (*TIT*=624°C; a similar idea was first proposed by Angelino [2] in an organic Rankine cycle with CF₄ as its working fluid), but here with some sharing of the working fluids, to take best advantage of the properties of available hardware for these cycles and of good exergy management in the cycles and heat exchangers. The fuel is a small fraction of the evaporated LNG, and the combustion oxidizer is pure oxygen produced in a conventional cryogenic vapor compression air separation plant. The system produces power, evaporates the LNG for further use while preventing more than 50% of the LNG exergy from going to waste during its evaporation, and produces liquefied CO₂ and water as the combustion products and liquid nitrogen and argon as the air separation products.

The topping Brayton cycle can be identified as 12→13→14→15→16→6→7→8→9→10→12. The bottoming Rankine cycle is 18→1→2→3→4→5→...→14→17→18. The LNG evaporation process is 20→21→22→23→24 & 25. The air separation process is 27→28 & 30. The process material products are liquid CO₂ (19), water (11), nitrogen and argon (30), and gaseous methane (24).

The **Brayton cycle** uses its exhaust gas heat to preheat its working fluid (CO₂) before entrance to the combustor (*B*), by *HE*₂, and then to evaporate the working fluid (CO₂) for the Rankine cycle by *HE*₁, the three-pass *HE*₂, and *HE*₃. The exhaust gas is then cooled further, by heating the LNG in *HE*₄, before compression by compressors *LC* and *HC* (this cooling reduces the compression work). The first compressor, *LC*, is used then to compress the working fluid to a pressure that would allow its condensation (in *HE*₅, the triple point of CO₂ is 5.18 bar and -56.6 °C), and some of the working fluid is withdrawn and first used to preheat combustion methane and oxygen in *HE*₇, and then condensed in *HE*₅. The remainder of the working fluid is compressed further in *HC* to the top pressure of the Brayton cycle, and then passed through the preheater *HE*₂ and combustor (*B*) before passing into the Brayton cycle turbine (*LT*). Assuming stoichiometric combustion, the exhaust gas of the Brayton cycle contains the combustion products CO₂ and H₂O through the path

both the thermal energy required for evaporation and the power that can be produced with the cryogenic cycle depend strongly on the LNG evaporation pressure. Different delivery pressures are typically made available at the receiving terminals: supercritical (typically 70 bar) for long distance pipeline network supply, and subcritical (typically 30 bar) for local distribution and power stations based on heavy-duty combined cycles [10]. In this paper, only the subcritical natural gas evaporation process (30bar) is considered, and the influence of different evaporation parameters will be investigated in forthcoming studies.

The placement of the heat exchangers in the cycle, and the choice of temperatures were made to reduce heat transfer irreversibilities. Furthermore, a combination of the higher -pressure (higher heat capacity) but lower mass flow rate fluid on the Rankine cycle side of the recuperators, with the lower-pressure (lower heat capacity) but higher mass flow rate fluid on the Brayton cycle side is also intended for reduction of irreversibilities.

THE CYCLE PERFORMANCE

The simulations were carried out using the commercial Aspen Plus [27] code. To simplify computation, it was assumed that the system operates at steady-state, the natural gas is pure methane, the combustion is stoichiometric with CO₂ and H₂O the only combustion products, no turbine blade cooling, and the stoichiometric amount of the water evacuated from the cycle does not contain dissolved CO₂. Besides, the outlet temperatures of the cold streams from HE₂ and HE₃ are set to be the same, i.e., $t_3=t_{16}=t_5$, since the calculation results suggest a worse efficiency for $t_3<t_{16}=t_5$. The most relevant assumptions for the calculations in this paper are summarized in Table 1.

The cycle minimal temperature is chosen as -70°C to avoid gas condensation, since the saturated temperature of CO₂ under ambient pressure (1 bar) is -78.4°C.

The First Law efficiency is calculated as the ratio between overall power output and heat input in the topping cycle [11]:

$$\eta_1 = W / (G_f \cdot H_u) \quad (1)$$

where W is the overall power output from the turbines, reduced by the power input to the compressors (LC and HC) and pumps (P_C , P_L), G_f is the fuel mass flow rate input. This cycle employs both fuel and LNG coldness (via its evaporation) as its input resources, but we have used only the fuel energy in the definition of η_1 , the First Law efficiency, because the LNG coldness is free, and it is actually of benefit to the user. Both input resources are, however, used in defining η_2 , the Second Law efficiency, which is the more appropriate criterion for performance evaluation than the fuel energy alone. It is defined here as the ratio between the net obtained and total consumed exergy

$$\eta_2 = W / (G_f \cdot H_u + G_L \cdot e_L) \quad (2)$$

assuming that the fuel exergy is approximately equal to its lower heating value H_u , G_L is the treated LNG mass flow rate, and e_L the exergy difference between the initial and the final states of the LNG evaporation process:

$$e_L = (h_{20} - h_{23}) - T_0(s_{20} - s_{23}) \quad (3)$$

and in the subcritical evaporation case (30.6 bar), which is about 560 kJ/kg_{LNG}, depends on the final temperature T_{23} .

For a given mass flow rate of the cycle working medium, the mass flow rates of needed fuel, of water and carbon dioxide recovered, and of LNG regasified can all be determined.

With 100 kg/s mass flow rate of CO₂ at the combustor inlet taken as reference, Table 2 summarizes the parameters, including temperature, pressure, flow rate and composition, of each stream for the subcritical pressure (30.6 bar) and temperature of 15 °C natural gas delivery. The mass flow rate of LNG regasified is found to be 54.69 kg/s, of which about 4% (2.2 kg/s) are sent to the combustor as fuel for the cycle; and the amount of water and CO₂ recovered are found to be 4.93 kg/s and 6.03 kg/s, respectively.

Table 1. Main assumptions for the calculation

Cycle parameter	High pressure P_h^* [bar]	150
	Intermediary pressure P_m [bar]	30
	Low pressure P_l [bar]	1
	CO ₂ condensation pressure [bar]	6.5
	CO ₂ condensation temperature [°C]	-48.8
	Lowest temperature t_{13} [°C]	-70
	Mass flow rate ratio of Brayton cycle R_g [%]	30
	Methane LHV H_u [kJ/kg]	50,010
Turbine	LT Inlet temperature t_6 [°C]	1,300
	Isentropic efficiency [%]	88
Compressor	Pressure ratio [%]	30.6
	Isentropic efficiency [%]	88
Combustor	Efficiency [%]	100
	Pressure loss [%]	3
Recuperation system	Water separator working temperature [°C]	10
	Heat exchangers Pressure loss [%]	2
ASU	Specific work for O ₂ production at 30.6 bar and 15 °C [kJ/kg O ₂]	900
LNG vaporization system	LNG pump efficiency [%]	77
	Pressure loss [%]	3
	Evaporation pressure [bar]	30.6
	Delivery temperature [°C]	15

*The highest pressure of the cycle is $P_1=156$ bar, 6 bar is for pressure losses in the heat exchangers

Table 2. The stream parameters of CO₂ cycle*

No.	t [°C]	P [bar]	G [kg/s]	Mole Composition		No.	t [°C]	P [bar]	G [kg/s]	Mole Composition		
				CO ₂	H ₂ O					CO ₂	CH ₄	O ₂
1	-44.8	156	70	1	0	16	623.5	30	30	1	0	0
2	201.6	153	70	1	0	17	53.8	6.565	76.03	1	0	0
3	623.5	150	70	1	0	18	-48.8	6.5	76.03	1	0	0
4	442.7	30.6	70	1	0	19	-44.8	156	6.03	1	0	0
5	623.5	30	70	1	0	20	-162	1	54.69	0	1	0
6	1300	29.1	110.96	0.9	0.1	21	-160.5	31.5	54.69	0	1	0
7	761.9	1.07	110.96	0.9	0.1	22	-126.7	31.2	54.69	0	1	0
8	656.2	1.05	110.96	0.9	0.1	23	-5	30.9	54.69	0	1	0
9	264.4	1.03	110.96	0.9	0.1	24	15	30.6	52.49	0	1	0
10	10	1.01	110.96	0.9	0.1	25	15	30.6	2.2	0	1	0
11	10	1.01	4.93	0	1	26	51.1	30	2.2	0	1	0
12	10	1.01	106.03	1	0	27	25	1	~37.76	air		
13	-70	1	106.03	1	0	28	15	30.6	8.76	0	0	1
14	61.1	6.63	106.03	1	0	29	51.1	30	8.76	0	0	1
15	201.6	30.6	30	1	0	30	/	/	~29.0	N ₂ , Ar,...		

* combustor inlet CO₂ mass flow rate of 100kg/s assumed as references

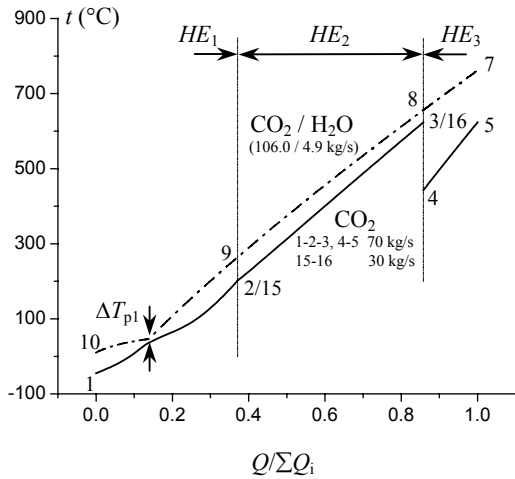


Fig. 3 t - Q diagram in CO₂ recuperation system

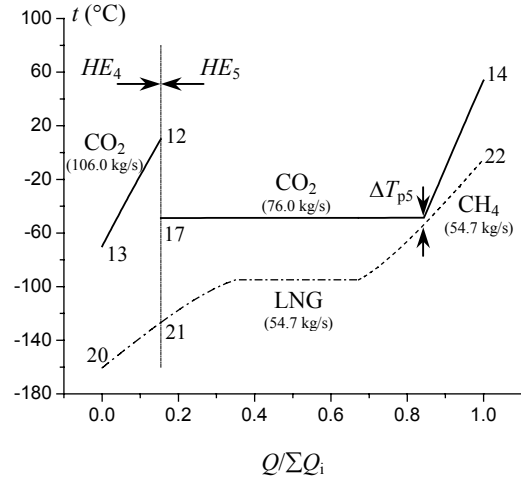


Fig. 4 t - Q diagram in LNG evaporation system

The computed performance of the cycle is summarized in Table 3 (first column). The total power produced is found to be 79.3 MW. Reduced by the power consumed for O₂ separation, which is roughly 7.9 MW (~10%), the net power output is 71.4 MW, resulting in a thermal efficiency (η_1) of 65% and exergy efficiency (η_2) of 51%. The difference between the efficiencies is due to their definition (Eqs (1) and (2)), where η_1 does not take into account the LNG coldness energy, while η_2 does. Consequently, such a plant would produce about 124 MWe if installed with the first Chinese LNG receiving terminal that has an import capacity of 3,000,000 t per year (95 kg/s).

Figures 3 and 4 are the t - Q diagrams for the recuperation system and the LNG evaporation system, respectively, where Q is the heat duty of a heat exchanger. Heat load distribution is not even among the different heat exchangers. The minimal temperature differences are present in HE₁ and HE₅. The pinch point in HE₁ appears at the point where the H₂O vapor contained in the hot LT exhaust stream begins to

condense. The minimal temperature difference, ΔT_{p1} , is 10 °C in this case and one way to raise it is to increase the flue gas temperature out of HE₁ (t_{10}), which will lead to more flue gas exhaust heat for LNG evaporation. The pinch point in HE₅ appears at the point where CO₂ begins to condense, and ΔT_{p5} is 5 °C in this calculation. Reducing the pinch point temperatures will increase the thermal performance, but larger heat transfer surface area and more equipment investment will be required.

The NG temperature at the HE₅ outlet is -5 °C, still cold enough to be used for local applications such as refrigeration and air conditioning. The total heat duty of HE₅ is 2.7MW, and if practical cooling can be accomplished up to $t_{24} = 5$ °C (rather than all the way to 15°C), a modest contribution of about 1.3MW of cooling can be obtained and added to the overall useful output of the system.

Table 3. Performance summary of different cycle configurations

	Base-case	No-LNG	reheat	intercooling	Reheat+intercooling
LT turbine work [MW]	80.9	80.5	44.6	81.3	44.9
MT turbine work [MW]	0	0	43.0	0	43.2
HT turbine work [MW]	15.0	15.1	16.3	14.6	16.3
LC compressor work [MW]	10.9	14.0	11.0	10.9	11.0
MC compressor work [MW]	0	13.7	0	0	0
HC compressor work [MW]	3.8	4.6	3.9	2.6	2.6
LNG pump work [MW]	0.5	0	0.5	0.5	0.5
CO ₂ pump work [MW]	1.4	1.3	1.4	1.4	1.4
Fuel/O ₂ expander	0	0	0.6	0	0.6
O ₂ separation work [MW]	7.9	7.7	8.4	8.1	8.7
Net power output [MW]	71.4	54.1	79.4	72.4	80.8
LNG mass flow rate [kg/s]	54.7	0	54.9	54.7	55.0
Fuel ratio [%]	4.02	/	4.28	4.14	4.42
Fuel energy input $G_f H_u$ [MW]	109.9	107.2	117.6	113.3	121.5
LNG exergy input $G_L e_L$ [MW]	30.5	0	30.7	30.9	31.0
First law efficiency [%]	65.0	50.5	67.5	63.9	66.5
Second law efficiency [%]	50.9	50.5	53.6	50.2	53.0

Table 4 shows the heat duties of the heat exchangers, and the estimated required heat exchanger surface areas. There are 7 heat exchangers in the system: recuperators (HE_1 , HE_2 , HE_3), LNG evaporators (HE_4 , HE_5 , HE_6) and a fuel/O₂ preheater, HE_7 . The recuperators are conventional heat exchangers with gas streams flow through both sides (ignoring the small amount water condensation in HE_1). HE_4 is a CO₂ gas-to-CH₄ liquid heat exchanger. As show in Fig. 4, HE_5 consists of two parts, in the first part it is exchanged between CO₂ gas and natural gas, in the second part CO₂ is condensed due to cooling by liquid, boiling, and gaseous CH₄ with an overall heat transfer coefficient estimated as 600 W/m²K [28]¹. In the calculation in Table. 4, the hot stream in HE_6 is assumed to be water with the inlet and outlet temperatures of 25 and 20°C, respectively. The total heat transfer area for the cycle is estimated to be 27,856 m², nearly 80% of which are the recuperators, and 20% the LNG evaporators, the latter accommodating about 30% of the total heat duty.

KEY PARAMETERS AND DISCUSSION

The key parameters that have influence on the cycle performance include the Brayton cycle mass flow rate ratio R_g , the low-pressure turbine inlet temperature t_6 , the cycle high and intermediary pressure level P_h and P_m .

The Brayton cycle mass flow rate ratio R_g is defined as the ratio of the mass flow rate of stream 16 (Fig.1) over that of the total CO₂ recycled in the system.

$$R_g = G_{16} / (G_5 + G_{16}) \quad (4)$$

¹ Precise determination of heat exchanger areas requires their detailed design specification. The estimates here are very rough, based on the assumption that the heat exchangers are of the shell-and-tube type, and using average typical overall heat transfer coefficient values for these heat exchanger processes and fluids as found in the process heat transfer literature [28]. Use of better heat exchangers, such as plate type, may reduce the required heat transfer area by as much as an order of magnitude.

If R_g equals to 1, the plant becomes a pure Brayton cycle, and less flue gas exhaust heat will be recovered in the recuperation system due to the sizable increase of the flue gas temperature at the inlet of the LNG evaporation system. This temperature equals to the sum of t_{15} and a temperature difference needed for heat transfer in HE_2 . At the other extreme, if $R_g = 0$, it is still a kind of quasi-combined cycle of a Brayton and a supercritical Rankine-like one, similar to the "MATIANT" cycle [25], and the higher heat capacity of the compressed liquid CO₂ will lead to a larger temperature difference between LT outlet flue gas and CO₂ entering the combustor, $t_7 - t_5$. Variation of R_g will thus not only change the flue gas heat distribution between the recuperation system and the LNG evaporation system, but also the heat balance inside the recuperation system itself. Calculation shows that both thermal efficiency and exergy efficiency increase by about 3 to 4 percentage points for every 100°C increase of t_6 (LT inlet temperature) or 20% increase of R_g . The specific power output w increases with the increase of t_6 and with the decrease of R_g .

A relatively high level for P_h and P_m was employed in some past studies of power cycles with CO₂ separation, for example, they are 240 bar and 60 bar, respectively in the "COOPERATE" [20, 22] and "COOLENERG" cycles [26], and 300 bar and 40 bar in the "MATIANT" cycle [25]. To relieve the technical problems incurred by these high pressure levels, the pressure P_h and P_m is chosen in our cycle to be 150 and 30 bar for the design point.

Computations show that both P_h and P_m have positive impact on the efficiencies and specific power output within certain calculation range ($P_m = 15 \sim 55$ bar and $P_h = 100 \sim 200$ bar). When P_h increases from 150 bar to 200 bar for $P_m = 25$ bar, the efficiencies increase by about 0.6 percentage point; and they increase by 1.7 percentage points when P_m increases from 15 to 25 bar for $P_h = 150$ bar. Obviously P_m has a more notable influence on the cycle thermal performance than P_h , clearly because the power output of the LP turbine is several fold bigger than that of the HP turbine. Increasing P_h and P_m results in the lowering of the HP and LP turbine flue gas temperature, respectively, leading to the drop of the pinch point temperature difference ΔT_{p1} , but it is not necessary to have very high values of P_h , since the HP turbine contributes less to the cycle power output.

Table 4. Heat exchanger surface area estimation

	Heat exchanger	Q [MW]	UA [kW/K]	U [27] [W/m ² K]	A [m ²]	A [%]	ΣA [m ²]
recuperators	HE_1	38.95	1005.76	99	10159.2	36.5	21,968
	HE_2	51.10	1011.75	93	10879.0	39.0	
	HE_3	14.93	86.47	93	929.8	3.3	
LNG evaporators	HE_4	6.71	59.63	99	602.3	2.2	5,632
	HE_5	36.86	1124.2	93/600	4645.6	16.7	
	HE_6	2.699	164.97	429	384.6	1.4	
fuel/O ₂ preheater	HE_7	0.50	23.73	93	255.1	0.9	255

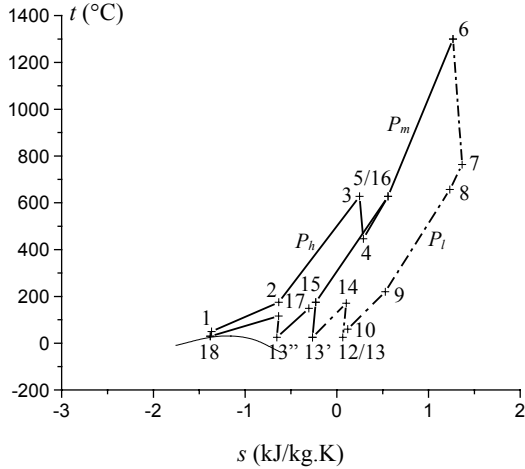


Fig.5 t - s diagram for CO₂ cycle without LNG

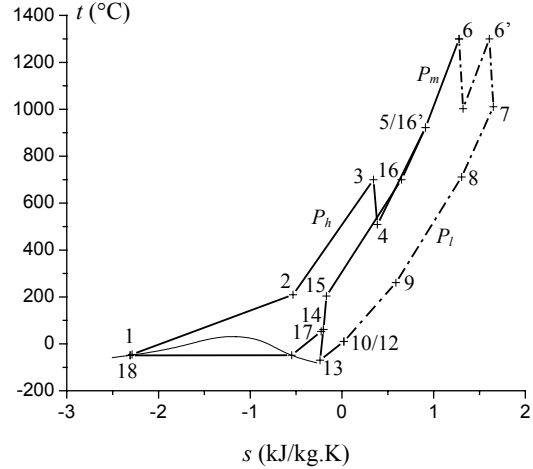


Fig.6 t - s diagram for CO₂ cycle with reheat

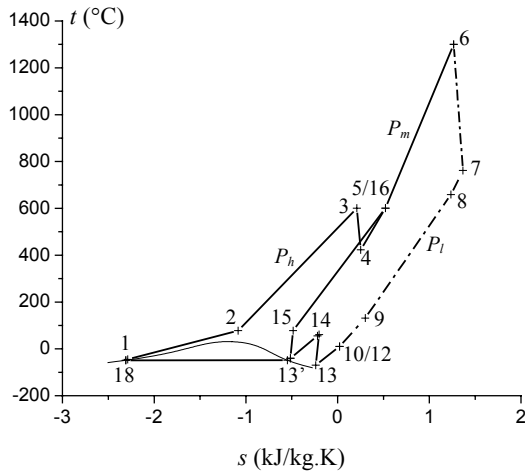


Fig.7 t - s diagram for CO₂ cycle with intercooling

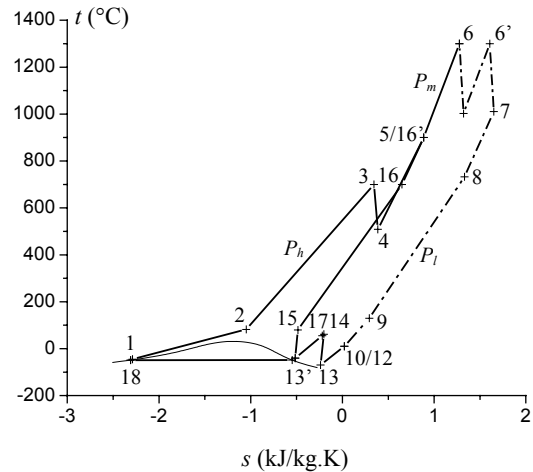


Fig.8 t - s diagram for CO₂ cycle with intercooling and reheat

Compared with the above-mentioned cycles, our cycle has two new features: first, while $R_g=0$ (no HC compressor) in those cycles, $R_g > 0$ in our cycle, which allows a much better turbine exhaust heat recovery in the recuperation system; second, integration here with the LNG evaporation process accomplishes CO₂ condensation at a much lower pressure. As a result, the computed thermal efficiency is as high

as 65% with the enabling technologies ($TIT=1300^\circ\text{C}$, $P_h=150$ bar and $P_m=30$ bar), which is about 10 to 15 percentage points of increment compared with the other above-mentioned cycles.

The typical cryogenic equipment for air separation consumes about 0.2~0.28 kWh of electric power per kilogram of O₂ separated [13], depending on the product purity, production capacity and so on.

It is found through the calculation that the power consumed for O₂ production is nearly 10% of the total power output, and every 10% reduction in the power needed for air separation will increase both efficiencies and power output by about 1.1%. Clearly, one way to improve system performance is to optimally integrate the air separation with the rest of the system.

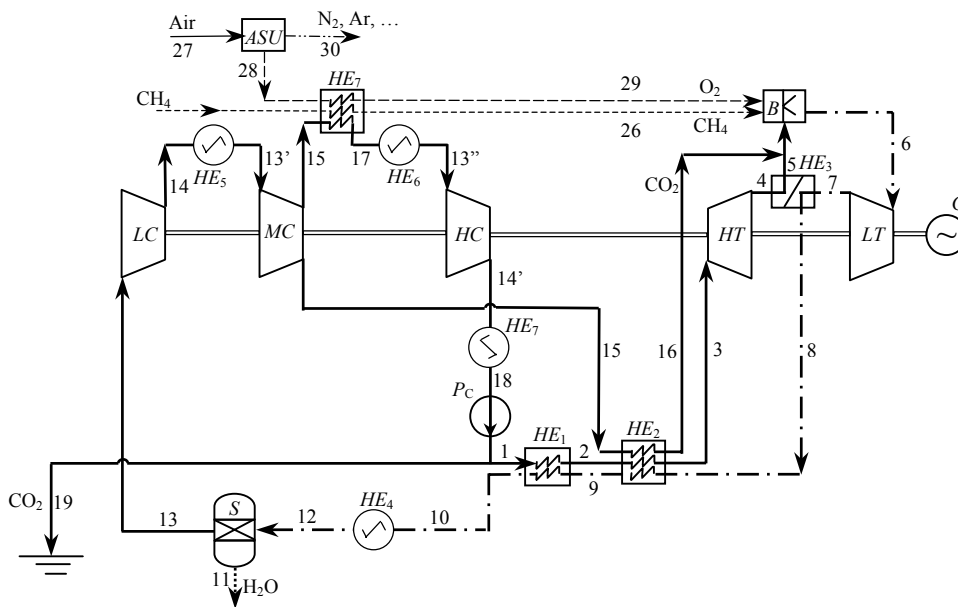
COMPARISON OF DIFFERENT CYCLE CONFIGURATIONS

With the base-case cycle described in Fig. 2 as reference, different system configurations were modeled and analyzed to further explore the effect of LNG exergy application and to examine the potential for performance improvement. These configurations include one where no LNG is used, one in which intercooling is used, one with reheat, and one with reheat and plus inter cooling. The corresponding *t-s* diagrams are shown in Figs.5-8, respectively.

Figures 9 and 10 show the cycle layout for the cycle without use of LNG coldness (no-LNG case), and the intercooling+reheat cycle, respectively. The reheat cycle is the combination of the left part of the schematic shown in Fig. 1 and the right part of that in Fig. 10. Similarly, the intercooling cycle is the combination of the right part of Fig. 1 and the left part of Fig. 10

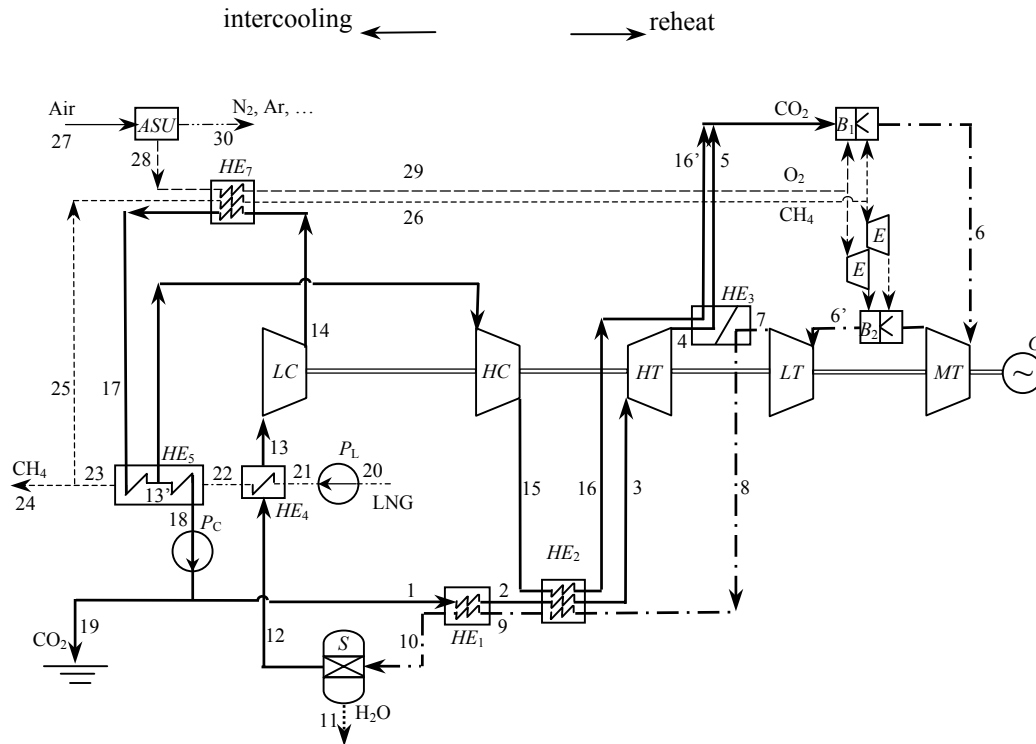
If LNG is not used for its coldness, as in [29], then a multi-stage compression process with intercooling 13→14→13'→15→17→13''→14'→18 (in Fig. 9) is adopted to bring the CO₂ up to a liquid state of 80 bar and 30 °C, instead of the CO₂ condensation process. This brings two advantages: elimination of non-condensable gases and the associated problems, and elimination of the need for a condenser. The cycle in Fig. 5 can hence be regarded as a combination of the “MATIANT” cycle and a CO₂ Brayton cycle with intercooling. Unlike all the other ones, this cycle works above the ambient temperature. It uses cold water as the intercooler coolant with the temperature varying from 15 to 20°C. The specific power output is about 76% of that of the base-case cycle, and it has the same thermal efficiency and exergy efficiency, which can reach 50%.

When reheat is employed, the low-pressure turbine outlet temperature *t*₇ can be raised significantly (to over 1000 °C, Figs. 6 and 8), and the turbine exhaust heat is large, able to raise temperature of the cold streams in *HE*₂ to a higher magnitude. However, for practical turbine materials, the high pressure turbine *HT* inlet temperature is restricted to 700°C in the calculations, and the excess amount of *LT* exhaust heat is used to raise the combustor inlet temperature to a higher level (point 5/16' in Figs. 6 and 8. The layouts of the cycles in Figs. 5-8 are somewhat different from that in Fig. 2 in terms of the number and the order of the heat exchangers).



ASU— Air separation unit B— Combustor G— Generator HE— heat exchanger
 LC/HC— Low / High pressure compressors LT/HT— Low / High pressure turbines
 P_C— Liquid CO₂ pump P_L— LNG pump S— water separator
 LNG is assumed to be CH₄ only
 ——— CO₂ H₂O LNG — — — CO₂ / H₂O
 - - - - - CH₄ ——— Air ——— O₂ ——— N₂, Ar, ...

Fig. 9 CO₂ cycle flow sheet without LNG cold exergy utilization



ASU— Air separation unit B— Combustor E— Fuel/O₂ expander G— Generator
 HE— heat exchanger LC/HC— Low / High pressure compressors
 LT/HT— Low / High pressure turbines P_C— Liquid CO₂ pump P_L— LNG pump
 S— water separator
 LNG is assumed to be CH₄ only
 ——— CO₂ H₂O - - - - -LNG - · - · - CO₂ / H₂O
 - - - - - CH₄ ——— Air - - - - -O₂ - · - · - N₂, Ar, ...

Fig. 10 CO₂ cycle flow sheet with reheat and intercooling

The performances are summarized and compared in Table 3 and Fig. 11-13 as functions of the intermediary pressure P_m . A fuel compressor (or expander) is needed when the combustion pressure in B is higher (or lower) than the natural gas delivery pressure. The efficiencies and power output are found to increase monotonically with P_m within the whole calculation range of P_m (from 20 to 40 bar), with a diminishing rate.

Employing reheat is seen to improve performance: both the thermal efficiency and exergy efficiency increase by 2 to 3 percentage points, and the specific power output increases by about 11%.

Employing intercooling increases the specific power output slightly, by 1.3% on average, but the thermal and exergy efficiency coincidentally drop by more and less than 1 percentage point, respectively. From Figs. 7 and 8, in the intercooling cycle, the working fluid temperature after compression is lower, but the hot stream temperature at the recuperator outlet t_{10} is fixed. This results in a lower combustor inlet temperature and thus more fuel is needed to raise the temperature to the desired turbine inlet temperature, which explains the efficiency drop. In the intercooling cycle, all the working

fluid needs to be cooled down by LNG after the first stage of compression (14→17→13' in Fig. 10). Therefore the amount of heat available in the LNG evaporation system will bring the evaporated natural gas to the near-ambient temperature, leaving no extra coldness for air conditioning.

The comparison between the reheat+intercooling cycle with the reheat cycle is similar to the comparison between the intercooling cycle with the base-case cycle. As known in general, incorporation of reheat or intercooling alone can increase the cycle power output, but not necessarily improve the efficiency, because of the higher turbine flue gas temperature in the cycle with reheat, or the lower compressor outlet temperature in the cycle with intercooling. It is also known that incorporation of recuperation (internal heat regeneration) may have other consequences. Unlike the situation in this paper, if the recuperator hot stream outlet temperature drops in the cycle with intercooling, it is possible to increase the overall efficiency as well.

Compared with the base-case cycle, the thermal efficiency of the no-LNG case is lower by nearly 15 percentage points, but their exergy efficiencies are about the same. Its exergy efficiency is between that

Table 5. Heat exchanger surface area comparison of different cycle configurations

	No LNG	reheat	intercooling	Reheat/intercooling	Base-case
Recuperators [m ²]	18,664	36,940	18,742.5	28,551.2	21,968
Others [m ²]	4,225.6	5,967.3	6,702.1	6,804.8	5,887.6
Total area ΣA [m ²]	22,889.6	42,907.3	25,444.6	35,356.0	27,855.6
$\Sigma A/\Sigma A_{ref}$ [%]	82.2	154.0	91.3	126.9	1

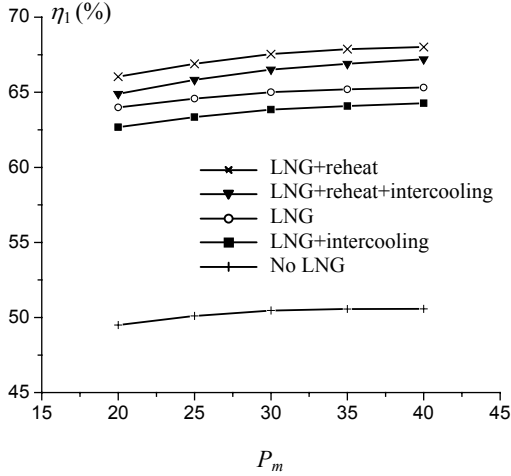


Fig. 11 The influence of P_m on thermal efficiency

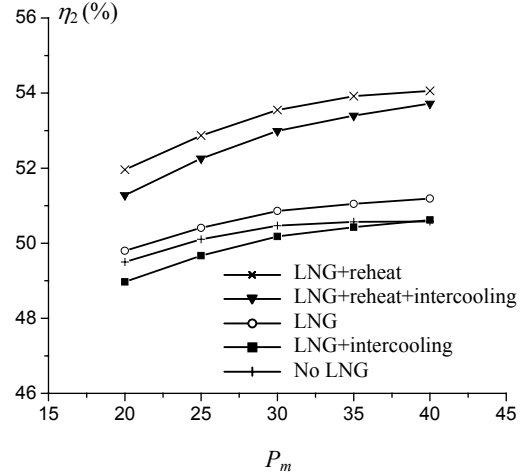


Fig. 12 The influence of P_m on exergy efficiency

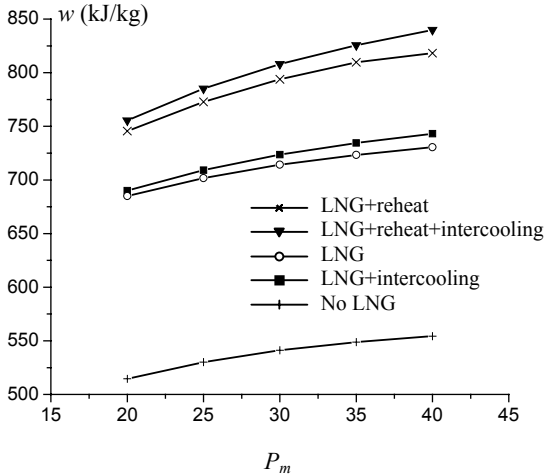


Fig. 13 The influence of P_m on specific power output

of the base-case cycle and the one with intercooling (Fig. 12). From Table 3, the LNG coldness contributes nearly 22% to the total base-case cycle exergy input, and it converts to power at almost the same efficiency as the fuel exergy does.

Among the cycle configurations studied in this paper, the reheat cycle has the highest efficiencies, while the reheat+intercooling cycle has the highest specific power output. It should, however, be noted that the recuperator material needs then to bear a temperature as high as 1000° C.

The heat exchanger surface areas for different cycle configurations are also estimated and compared in Table 5. Differences mainly exist in the recuperation system. Compared with

the base-case cycle, it was found that reheat cycle requires 54% additional heat transfer area, and the no-LNG cycle and intercooling cycle require 18% and 9% less, respectively.

CONCLUSIONS

A novel power cycle producing zero CO₂ emission by integration of LNG cryogenic exergy utilization is proposed and thermodynamically modeled. The main merits of the system include:

- 1) good thermodynamic performance, with the energy and exergy efficiencies reaching 65% and 51%, respectively, using conventional technologies, despite the power consumed for air separation;
- 2) negligible release of pollutants to the environment;
- 3) removal of high pressure liquid CO₂ ready for sale or disposal;
- 4) valuable byproducts: condensed water, liquid N₂ and Ar;
- 5) full exploitation of the LNG evaporation process.

The influences of some key parameters on the cycle performance, including the Brayton cycle mass flow rate ratio, the low-pressure turbine inlet temperature and pressure levels, are discussed. Thermal efficiency and exergy efficiency increase by about 3 to 4 percentage points for every 100°C increase of t_6 (LT inlet temperature) or 20% increase of R_g . The specific power output w increases with the increase of t_6 and with the decrease of R_g . Both P_h and P_m have positive impact on the efficiencies and specific power output within the calculation range; and P_m has a more notable influence on the cycle thermal performance than P_h . It is also found that every 10% reduction in the power needed for air separation will increase both efficiencies and power output by about 1.1%.

The total needed heat exchanger area is about 390 m²/MWe for the base-case cycle, ~75% of which are the recuperators HE_1 and HE_2 . Employing larger heat transfer temperature differences can effectively reduce the heat transfer surface area, but will lead to a reduction of

thermal efficiency. A formal thermoeconomic optimization is obviously called for. The pinch point temperature difference in the recuperation system is one of the main constraints to performance improvement, its influence and parameter optimization calls for further study.

Among the different cycle schemes investigated, it was found that highest efficiencies' improvement over the base-case can be obtained by employing reheat but only by 2 to 3 percentage points, and this would also increase the specific power output by more than 10%. The major practical restrictions to employing reheat is the high recuperator inlet temperature for reheat cycle, and a 54% increase in the overall heat transfer surface. Compared with the base-case, incorporation of intercooling lowers efficiencies and slightly increases power output. If no LNG coldness is used, the cycle operates in the same temperature range as conventional power plants do, the required heat exchange area is reduced by 18% (only), the specific power output is reduced by one quarter, and the efficiency can reach 50%, about 15 percentage points lower than that of the base-case cycle.

Based on this analysis, the proposed base-case plant (which wasn't optimized yet) would produce 124MWe if installed with the first LNG terminal in China that has an import capacity of 3,000,000 t/yr, and the capacity can be increased up to 137MWe and 140MWe for reheat cycle and reheat/intercooling cycle, respectively.

ACKNOWLEDGEMENT

The authors gratefully acknowledge the support of the K. C. Wong Education Foundation, Hong Kong; the Chinese Natural Science Foundation Project (No. 50006013 & 59925615), and the Chinese National Key Fundamental Research Project (No. G1999022302).

REFERENCES

- [1] Karashima, N., and Akutsu, T., 1982, "Development of LNG Cryogenic Power Generation Plant", Proceedings of 17th IECEC, pp. 399-404.
- [2] Angelino, G., 1978, "The Use of Liquid Natural Gas as Heat Sink for Power Cycles", ASME Journal of Engineering for Power, **100**, pp. 169-177.
- [3] Kim, C. W., Chang, S. D., Ro, S. T., 1995, "Analysis of the Power Cycle Utilizing the Cold Energy of LNG", International Journal of Energy Research, **19**, pp. 741-749.
- [4] Najjar, Y. S. H., Zaaout, M. S., 1993, "Cryogenic Power Conversion with Regasification of LNG in a Gas Turbine Plant", Energy Convers. Mgmt, **34**, pp. 273-280.
- [5] Wong, W., 1994, "LNG Power Recovery", Proceedings of the Institution of Mechanical Engineers, Part A: Journal of Power and Energy, **208**, pp. 1-12.
- [6] Zhang, N., and Cai, R., 2002, "Principal Power Generation Schemes with LNG Cryogenic Exergy", Proceedings of ECOS'02, Berlin, Germany, pp. 334-341.
- [7] Krey, G., 1980, "Utilization of the Cold by LNG Vaporization with Closed-Cycle Gas Turbine", ASME Journal of Engineering for Power, **102**, pp. 225-230.
- [8] Agazzani, A., Massardo, A. F., 1999, "An Assessment of the Performance of Closed Cycles with and without Heat Rejection at Cryogenic Temperatures", ASME Journal of Engineering for Gas Turbines and Power, **121**, pp. 458-465.
- [9] Deng, S., Jin, H., et al, 2001, "Novel Gas Turbine Cycle with Integration of CO₂ Recovery and LNG Cryogenic Exergy Utilization", Proceedings of ASME IMECE 2001.
- [10] Chiesa, P., 1997, "LNG Receiving Terminal Associated with Gas Cycle Power Plants", ASME paper 97-GT-441.
- [11] Desideri, U., and Belli, C., 2000, "Assessment of LNG Regasification Systems with Cogeneration", Proceedings of TurboExpo 2000, Munich, Germany, 2000-GT-0165.
- [12] Kim, T. S., and Ro, S. T., 2000, "Power Augmentation of Combined Cycle Power Plants Using Cold Energy of Liquefied Natural Gas", Energy, **25**, pp. 841-856.
- [13] Velautham, S., Ito, T., Takata, Y., 2001, "Zero-Emission Combined Power Cycle Using LNG Cold", JSME International Journal, Series B. Fluids and Thermal Engineering, **44**, pp. 668-674.
- [14] Riemer, P., 1996, "Greenhouse Gas Mitigation Technologies, an Overview of the CO₂ Capture, Storage and Future Activities of the IEA Greenhouse Gas R&D Program", Energy Conversion and Management, **37**, pp. 665-670.
- [15] Haugen, H. A., Eide, L. I., 1996, "CO₂ Capture and Disposal: the Realism of Large Scale Scenarios", Energy Convers. Mgmt, **37**, pp. 1061-1066.
- [16] Yantovski, E. I., Zvagolsky, K. N., Gavrilenko, V. A., 1992, "Computer Exergonomics of Power Plants without Exhaust Gases", Energy Convers. Mgmt, **33**, pp.405-412.
- [17] Shao, Y., Golomb, D., 1996, "Power Plants with CO₂ Capture Using Integrated Air Separation and Flue Gas Recycling", Energy Convers. Mgmt, **37**, pp. 903-908.
- [18] Shao, Y., Golomb, D., Brown, G., 1995, "Natural Gas Fired Combined Cycle Power Plant with CO₂ Capture", Energy Convers. Mgmt, **36**, pp. 1115-1128.
- [19] Wall, G., Yantovski, E., Lindquist, L. and Tryggstad, J., 1995, "A Zero Emission Combustion Power Plant for Enhanced Oil Recovery", Energy, **20**, pp. 823-828.
- [20] Yantovski, E. I., 1996, "Stack Downward Zero Emission Fuel-Fired Power Plants Concept", Energy Conversion and Management, **37**, pp. 867-877.
- [21] Yantovski, E. I., Gorski, J., 2000, "Further Elaboration of Quasi-combined Zero-Emission Power Cycle", Proceedings of ECOS 2000, Enschede, Netherlands, pp. 1083-1092.
- [22] Yantovski, E. I., Zvagolsky, K. N., and Gavrilenko, V. A., 1995, "The COOPERATE-Demo Power Cycle", Energy Conversion and Management, **36**, pp. 861-864.
- [23] Mathieu, P., Dubuisson, R., Houyou, S., Nihart, R., 2000, "A Quasi Zero Emission O₂/CO₂ Combined Cycle", Proceedings of ECOS 2000, Enschede, Netherlands, pp. 1071-1081.
- [24] Fioravanti, A., Lombardi, L., and Manfrida, G., 2000, "An Innovative Energy Cycle with Zero CO₂ Emissions", Proceeding of ECOS'2000, Eschende, Netherlands, pp. 1059-1070.
- [25] Mathieu, P., and Nihart, R., 1999, "Zero-Emission MATIANT Cycle", Journal of Engineering for Gas Turbines and Power, Transactions of the ASME, **121**, pp. 116-120.
- [26] Staicovici, M. D., 2002, "Further Research Zero CO₂ Emission Power Production: the 'COOLENERG' Process", Energy, **27**, pp. 831-844.
- [27] Aspen Plus®, Aspen Technology, Inc., Version 11.1, <http://www.aspentech.com/>.
- [28] Cai, R., 1998, "A new Analysis of Recuperative Gas Turbine Cycles", Proceedings of the Institution of Mechanical Engineers, Part A: Journal of Power and Energy, **212**, pp. 289-296.
- [29] Mathieu, P., and Nihart, R., 1999, "Sensitivity Analysis of the MATIANT Cycle", Energy Conversion and Management, **40**, pp. 1687-1700.